PLUME EFFECTS ON THE FLOW AROUND A BLUNTED CONE
AT HYPERSONIC SPEEDS

P. Atcliffe, D. Kumar & J.L Stollery
College of Aeronautics
Cranfield Institute of Technology
Cranfield, Bedford, U.K.
MK43 0AL

ABSTRACT

Tests at M = 8.2 show that a simulated rocket plume at the base of a blunted cone can cause large areas of separated flow, with dramatic effects on the heat transfer rate distribution. The plume has been simulated by solid discs of varying sizes or by an annular jet of gas. Flow over the cone without a plume is fully laminar and attached. Using a large disc, the boundary layer is laminar at separation at the test Reynolds number. Transition occurs along the separated shear layer and the boundary layer quickly becomes turbulent. The reduction in heat transfer associated with a laminar separated region is followed by rising values as transition occurs and the heat transfer rates towards the rear of the cone substantially exceed the values obtained without a plume. With the annular jet or a small disc, separation occurs much further aft, so that heat transfer rates at the front of the cone are comparable with those found without a plume. Downstream of separation the shear layer now remains laminar and the heat transfer rates to the surface are significantly lower than the attached flow values.

INTRODUCTION

A rocket exhausting from the rear of a vehicle can severely modify the flow in the base region. In particular, exhaust jets can expand so spectacularly at high altitude that flow separation is induced over the rear of the body ahead of the jet plume.

The flow over a blunted cone at M_∞ = 8.2 was studied in the experiments described here. The exhaust plume was simulated initially by attaching one of a number of solid discs of varying sizes to the base of the cone; in later tests, a radial jet of gas (air, helium or argon) was used to more closely model a real plume. Platinum thin film gauges measured the heat transfer rates on the cone surface and schlieren photographs showed the separated flow patterns.

EXPERIMENTAL DETAILS

The Hypersonic Gun Tunnel

A sketch of the tunnel is shown in figure 1. Measurements of reservoir pressure, made at the end of the barrel, and stagnation pressure in the test section, confirm calibrations made earlier.[1,2]

The test conditions, based on the assumption of perfect gas flow, were:

M_∞ = 8.2, Re_∞ = 2.37 x 10^5 per inch

p_∞ = 0.138 psia, Po_∞ = 1580 psia

T_∞ = 89.3K, To_∞ = 1290K

The useful running time of the tunnel was approximately 25ms.

The Blunted Cone Model

A 7° semi-angle blunted cone model was manufactured from "Macor" machinable glass-ceramic and instrumented with nine platinum thin film gauges as shown in Figure 2. The gauges were painted directly onto the cone surface and baked. Conductive paint provided the electrical connection between the gauges and brass contact rods which, as shown in the figure, ran transversely through the model. The rods were connected to leads which were taken away internally and out through the support sting to the data acquisition system. The gauges were calibrated by immersing the model in a heated oil bath and recording the variation of electrical resistance with temperature over a range of approximately 20°C.

The discs simulating the plume were made from aluminium and mounted flush against the base of the cone. Later tests were made using a plenum chamber fitting mounted on the support sting aft of the model. The exhaust gas (air, argon or helium) was fed to the chamber from an external supply via four tubes attached to the sting, as shown in figure 2b. The large pressure ratios used, typically between 40 and 250, choked the slot between the base and the plenum chamber, so that a radial jet sheet exhausted into the free stream. The width of the slot could be varied between tests.

Heat Flux Measurement

The thin film gauges and data acquisition system produced records of electrical signals which were proportional to the temperature variation of each gauge with time. These signals must be integrated to find the heat transfer rates which are of interest. Two methods were used during these tests.

The first method used an analogue network to convert the signal from each gauge into one proportional to the variation of heat transfer rate with time. Such a network is described by Meyer[3], and his design was adopted with circuit components chosen to suit the running time of the gun tunnel.

The second method involved numerical integration of the temperature signals, which were either stored digitally on floppy discs or plotted out into hard-copy form. Data points taken from either representation were used to calculate heat transfer rates using the method described by Schultz and Jones[4].

Both methods were used initially, but the analogue networks began to deteriorate and become unreliable with age, so that most of the results presented below were found using the numerical technique.

RESULTS AND DISCUSSION

Blunted Cone

Figure 3 is a schlieren photograph of the flow around the cone when no exhaust plume is present. The boundary layer is laminar and attached along the full length of the model and the contour of the bow shock is smooth and continuous. As will be seen later, a turbulent layer can generate waves of sufficient strength to visibly perturb the shock shape.

Non-dimensional rates of heat transfer to the cone surface, as measured by the thin film gauges, are plotted in the form of Stanton number vs free-stream Reynolds number based on axial distance x. Figure 4 shows the heat flux distribution found by Sperinck[5] in an earlier series of tests with an identical model in the Cranfield gun tunnel. The theoretical value for the stagnation point Stanton number is 0.029, so the figure shows how rapidly the distribution falls around the nose of the cone: by the first measuring station, St is less than 10% of the stagnation value. Figure 4 also presents a theoretical estimate of the heat transfer rate distribution on a sharp cone, calculated using the Mangler transformation on theoretical flat plate values, as described by Crabtree, Dommett and Woodley[6]. Over the instrumented region of the model, both curves show the heat transfer dropping as $Re_x^{-1/2}$, which confirms the laminar nature of the flow.

Blunted Cone With Disc

Discs ranging in size from 1.25 to 2.1 times the base diameter of the cone were fitted at the rear of the model to simulate an underexpanded exhaust plume. Schlieren photographs of the flow over the model showed that the presence of the disc caused separation along a large part of the length of the cone. Figures 5 and 6 illustrate the two extremes of the range of disc sizes tested, with d/d_B values of 1.25 and 2.1 respectively.

With the smallest disc fitted (figure 5), laminar separation occurs at an x/L value of slightly under 0.6, followed by a laminar shear layer. Towards the rear of the separated zone, the shear layer thickens, the edge becomes ragged and waves can be seen emanating from the boundary of the separated region.

As the size of the disc increases, the separation position moves forward, as shown in figure 7. The shear layer remains laminar initially but soon become wavy and appears turbulent. With the largest disc (figure 6), the detached region begins very close to the nose, separation occurring at x/L ≈ 0.07. The photograph indicates a laminar shear layer rapidly becoming transitional and then turbulent over most of the length of the cone.

Heat transfer measurements were made using discs of size d/d_B = 1.25, 1.4 and 2.1. Results from the latter two cases are shown in figure 8 together with the cone-only distribution. Results from the first case are described later. It is expected that heat transfer in a region of detached laminar flow will be reduced by comparison with that in an attached laminar region. This may be seen by comparing the appropriate portions of the heat flux distributions. In the case of the larger disc (d/d_B = 2.1), separation has already occurred ahead of the first thin film gauge, so that the Stanton number at that point is considerably less than that found in the cone-only case. This is followed by a rising heat transfer rate as the free shear layer undergoes transition to turbulent flow, so that the value of St exceeds that of the attached flow case over more than half the length of the cone.

For the smaller disc (d/d_B = 1.4), separation takes place at about x/L = 0.3. Ahead of this station the Stanton number is comparable with that of the cone-only case. After separation, the detached laminar region exhibits a drop in St, followed by a sharp increase as the shear layer becomes turbulent.

These trends agree with those obtained by Needham[7] and Holden[8] in their respective studies of (i) flow past a compression corner and (ii) flow over a step on a flat plate. In both cases, significant reductions in heat transfer rate were found in regions of laminar separated flow with a subsequent rapid rise as transition occurs.

The flow past the cone-disc configuration is reminiscent of that over a spiked body where the bow shock ahead of a blunt body interacts with the boundary layer growing along the spike. The shock wave causes separation and the separation point moves to near the tip of the spike, with dramatic changes to the effective shape of the body. In our tests, the blunted cone represents the spike and the disc, the blunt body. Adding a disc effectively changes the body shape from the initial slender blunted cone to a less-slender cone of semi-angle θ given approximately by tan θ = R/L.

Blunted Cone with Radial Jet

Initial tests with the external gas supply examined the effects of slot size and gas pressure. Air jets with total pressures ranging from 1 to 6 atmospheres were used with slot widths between 0.5 and 4.0 mm. For comparison, the static pressure on the surface of the cone for attached flow was calculated to be about 0.025 atmospheres.

The effect of gap size was found to be small over most of the range of widths tried, and a standard slot size of 4 mm (later, 4.5 mm) was adopted for the remainder of the tests. For a given gap width, the extent of the separated region increased with jet total pressure, as expected, and the variation of separation length with jet pressure for one slot size is included in figure 7. The curve shows that for a supply pressure difference above one atmosphere the increase of separated length with pressure is approximately linear. Clearly, a very high jet pressure would be needed to cause separation near the nose as was achieved with discs with values of d/d_B greater than about 1.6.

Tests were made using helium and argon as the exhaust gas to assess the effects of using a foreign gas and of gases of differing molecular weights. The results were perhaps surprising: compared to an air jet of the same supply pressure, both argon and helium produced slightly larger separated regions. Assuming choked flow with the gas issuing at a Mach number of one, the jet velocity for helium is three times that of air but the density is only 1/7th. Thus, the mass flow rate for helium is lower than for air, but the momentum and energy fluxes are greater.

For argon, the jet speed is less than that of air by some seven percent, but the density is greater by 38 percent, so that the mass, momentum and energy fluxes all exceed those of air. This would appear to imply that the momentum or energy fluxes are of more importance in determining the extent of separation, but a more careful analysis of duct losses and actual exit conditions would be needed to determine the merits of foreign gas injection.

Heat transfer measurements were made for the case of an air jet with a supply pressure of 75 psig (6.10 atmospheres total pressure) exhausting through a 4.5 mm gap. Figure 9 is a Schlieren photograph of the flow past the model and plume. Separation occurs at $x/L \approx 0.45$, after which the by-now familiar pattern of an initially laminar shear layer undergoing transition to turbulent flow over the rear of the body may be seen. The flow is very like that seen in figure 5 for the model with a small disc ($d/d_B = 1.25$), and the separation positions are similar

Nevertheless, a gas jet will entrain flow in a manner which a solid disc of any size cannot emulate. Hence, for a given separation station, one would expect the shape of the conical separated zone to be more acute with jet-induced separation. The experimental data supports this view.

The flow pattern within the separated region is another example of the difference between using a solid disc and a gas jet to simulate an exhaust plume. Figure 10 shows sketches of patterns proposed by the authors for the mean flow in each case. With a solid disc mounted at the rear of the cone, the separated flow re-attaches itself to the surface of the disc, producing a region of contraflow as one might expect. The situation is more complex with the gas jet: the boundary conditions have changed, and the requirement for the flow near the plume boundary to move outwards with the jet gas necessitates the presence of a pair of counter-rotating vortices to satisfy both that requirement and the need for an area of reversed flow.

The similarity between the air jet and small disc cases is also seen in the heat flux distributions shown in figure 11. Since separation does not occur in either case until well back along the cone body, the Stanton numbers found on the first forty percent of the length of the model are comparable to those obtained for the cone alone. For the air jet case, separation occurs just aft of this point and the heat transfer rate drops dramatically in the region of detached laminar flow, before rising slowly over the rear of the cone as the shear layer appears to become turbulent.

The small-disc case exhibits like behaviour, although separation is slightly further to the rear. Thus, the locations at which the heat flux distribution decreases sharply and then rises gently are a short distance behind those found using the air jet.

As noted previously, the heat transfer rate distributions shown in figures 8 and 11 agree with similar measurements made in other investigations. Figure 12 shows the distribution found by Holden[8] when studying the flow past a step on a flat plate at $M_\infty = 10$. The step causes laminar separation on the plate and the heat transfer distribution reflects this behaviour. The separated shear layer subsequently undergoes transition, and the initial drop in Stanton number is followed by a rapid rise as the layer becomes turbulent.

General Comments

Flow steadiness is an important factor in any experiment performed in an intermittent facility like a gun tunnel. In the case of these tests, comparison of schlieren photographs of nominally identical tunnel runs produced confidence that the flow could be considered as reasonably steady. There was inevitably some variation between runs, as indicated by the scatter in the heat flux results, but the photographs showed the flow patterns to exhibit satisfactory repeatability.

It is also worthy of note that the flow past the cone and simulated plume was not perfectly axi-symmetric. It was consistently found during examination of Schlieren photographs that separation on the underside of the model occurred slightly further forward than that on the top side. This indicates that there is a three-dimensional nature to the flow, and the locus of separation points around the surface of the cone is not the circular cross-section of the body expected in perfect axi-symmetric flow.

CONCLUSIONS

The flow over a slender blunted cone at $M_\infty = 8.2$ and $Re_\infty = 2.37 \times 10^5$ per inch was attached and laminar.

Simulating an exhaust plume from the base of the cone, either by fitting a solid disc or by providing a radial gas jet from a choked slot, produces widespread separation. The larger the disc, or the greater the pressure of the gas jet, the further forward the point of separation moves.

The shear layer is laminar at separation but can undergo transition to fully turbulent flow before reaching the base of the cone and the "plume".

The effect of the laminar shear layer is to decrease the heat transfer rate, by comparison with that for the cone alone, over the surface immediately behind the separation point. As the layer becomes turbulent, the heat transfer rate begins to increase and can exceed that of the cone by itself by a considerable margin. Whether the heat flux on the rear of the cone with plume is greater or less than that of just the cone depends on the extent of the separated region: the further forward the separation point, the higher the heat transfer to the rear of the cone.

ACKNOWLEDGEMENTS

NOTATION

C_p	specific heat at constant pressure
d	disc diameter $= 2R$
d_B	base diameter of cone
L	cone length (fig.2a)
L_{sep}	length of separated region on cone
M_∞	Mach number in the test section
p_∞	static pressure in test section
$P_{o\infty}$	reservoir pressure
Pr	Prandtl number (taken as 0.72 here)
$\dot{q}$	heat transfer rate
$\dot{q}_{fp}$	q on flat plate
R	disc radius (fig.2a)
Re_∞	Reynolds number per unit length
	$= \rho_\infty u_\infty / \mu_\infty$
Re_x	Reynolds number $= \rho_\infty u_\infty x/\mu_\infty$
r	recovery factor $= \sqrt{Pr}$
St	Stanton number $= \dot{q}/\rho_\infty u_\infty C_p (T_{aw} - T_\infty)$
T_{aw}	adiabatic wall temperature
	$= T_\infty (1 + r . \frac{\gamma-1}{2} M_\infty^2)$
T_∞	temperature in test section
$T_{o\infty}$	reservoir temperature
u_∞	velocity in test section
x	axial distance
γ	ratio of specific heats
μ_∞	viscosity in test section
ρ_∞	density in test section

REFERENCES

1. Stollery, J.L., Maull, D.J. and Belcher, B.J. "The Imperial College gun tunnel". J.Royal Aeronautical Society, Volume 64, No.589, p24 (1960).

2. Needham, D.A. "Progress report on the Imperial College hypersonic gun tunnel". Aerodynamics Report No. 118, Imperial College, London (1963).

3. Meyer, R.F. "Further comments on analogue networks to obtain heat flux from surface temperature measurements". National Research Council of Canada Aeronautical Report LR-375 (1963).

4. Schultz, D.L. and Jones, T.V. "Heat transfer measurements in short-duration hypersonic facilities". AGARDograph AG-165 (1973).

5. Sperinck, N.P.B. "The simulation of rocket plume effects on a blunted conical body". M.Sc thesis, College of Aeronautics, Cranfield Institute of Technology (1989).

6. Crabtree, L.F., Dommett, R.L., and Woodley, J.G. "Estimation of heat transfer to flat plates, cones and blunt bodies". RAE Technical Report No. 65137 (1965).

7. Needham, D.A. "Laminar separation in hypersonic flow". Ph.D thesis, Imperial College, University of London (1965). See also: "A heat transfer criterion for the detection of incipient separation in hypersonic flow". AIAA Journal, Volume 3, No.4, p781, April 1965.

8. Holden, M.S. "Heat transfer in separated flows". Ph.D thesis, Imperial College, University of London (1963). See also: "Leading-edge bluntness and boundary-layer displacement effects on attached and separated laminar boundary layers in a compression corner". AIAA Paper 68-68, 6th Aerospace Sciences Meeting, New York (1968).

$$M_\infty = 8.2 \quad , \quad Re_\infty = 9.34 \times 10^6 \text{ per metre} \quad , \quad T_{o\infty} = 1290°K \quad , \quad P_{o\infty} = 108 \text{ Atmospheres}$$

$$\text{Running time} = 25 \text{ msec.}$$
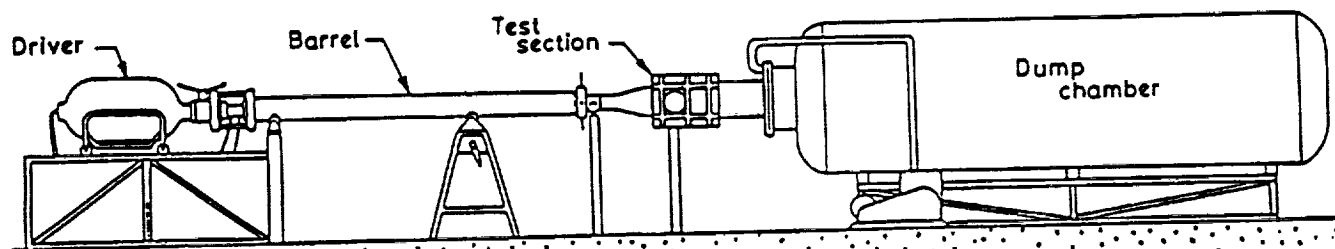
Fig 1.   Sketch of the gun tunnel

Thin film heat transfer gauge
Semi-vertex angle = 7°
Nose radius = 0.12 in
2.5 in dia. Disc
2.0 in dia. Disc
R
1.2 in dia.
Contact rod
Leads
L = 4 in
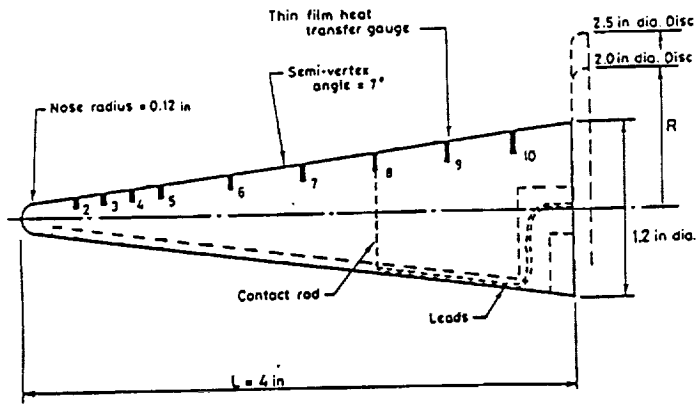
Fig 2a. Blunted cone model showing discs at the base
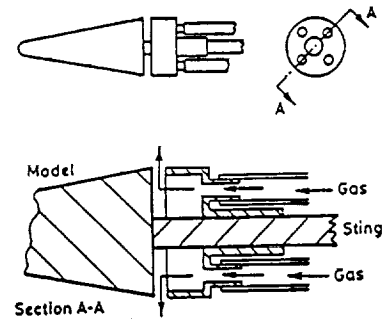

Model
Gas
Sting
Gas
Section A-A

Fig 2b. Same model with adaptor to give a radial jet.

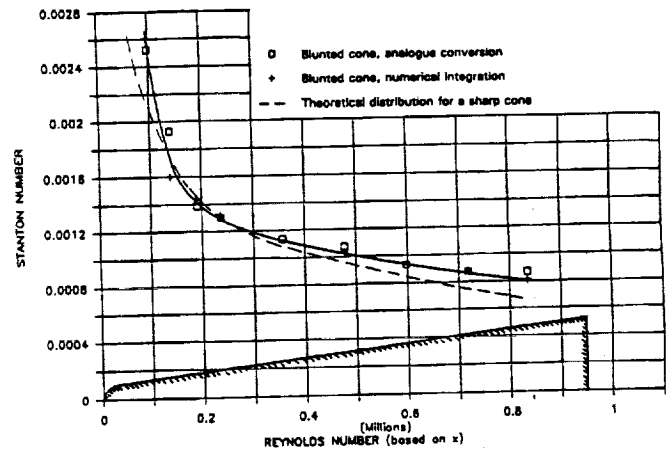Figure 3. Schlieren photograph of flow past the blunted cone.

□ Blunted cone, analogue conversion
+ Blunted cone, numerical integration
— — Theoretical distribution for a sharp cone

STANTON NUMBER
REYNOLDS NUMBER (based on x)
(Millions)

Figure 4. Heat transfer rate distribution on the surface of blunted and sharp cones.
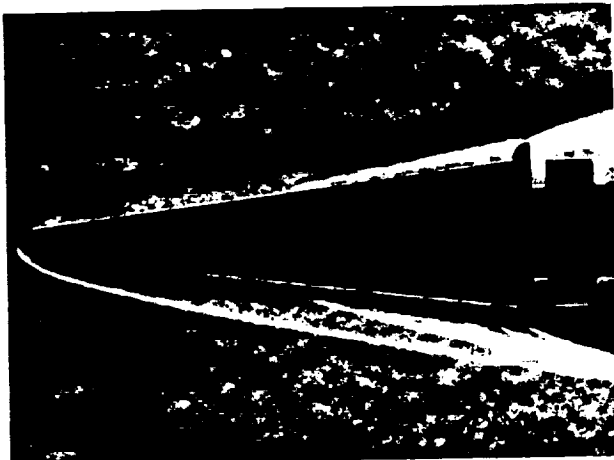
Figure 5. Schlieren photograph of flow past the blunted cone with a small disc (d/d_B = 1.25) at its base.
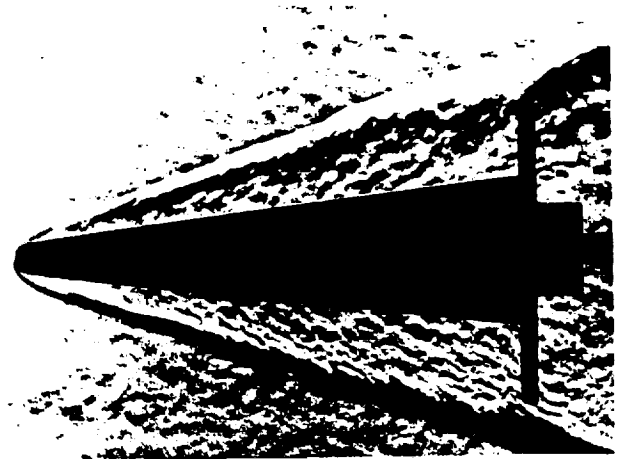
Figure 6. Schlieren photograph of flow past the blunted cone with a large disc (d/d_B = 2.1) at its base.
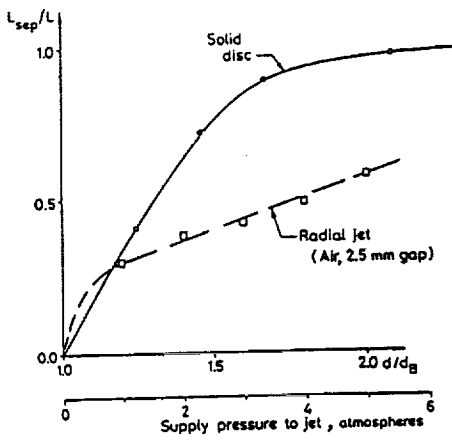
Figure 7. Movement of separation position with disc size and jet pressure.
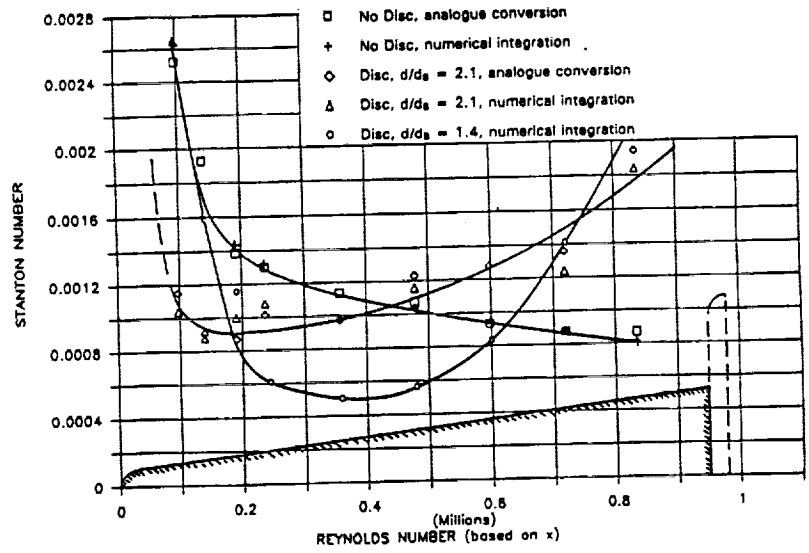
Figure 8. Effect of large- and medium-diameter discs on heat transfer to cone surface.
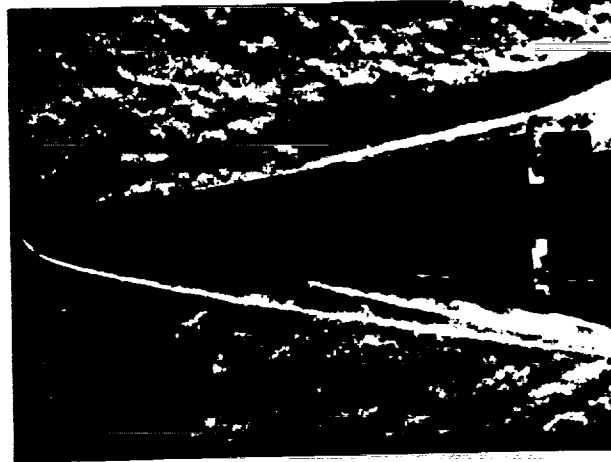
Figure 9. Schlieren photograph of flow past the blunted cone with an annular air jet (6.1 atm total pressure, 4.5 mm gap) at its base.

(a)   Large solid disc
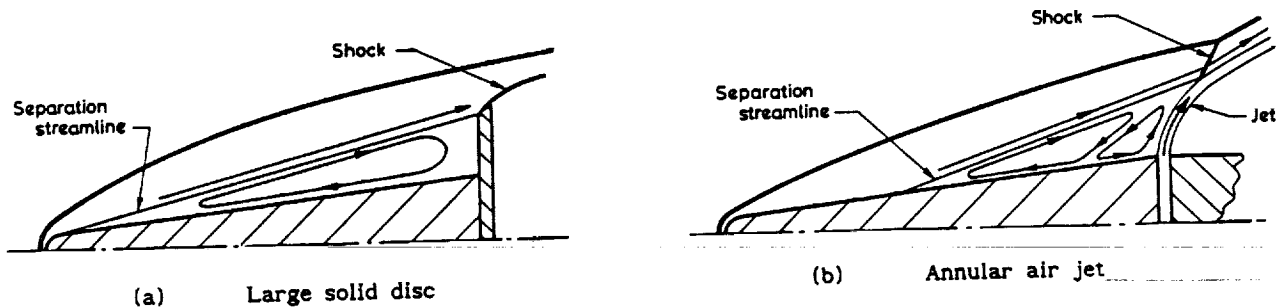
(b)   Annular air jet

Figure 10. Suggested flow patterns in separated regions.
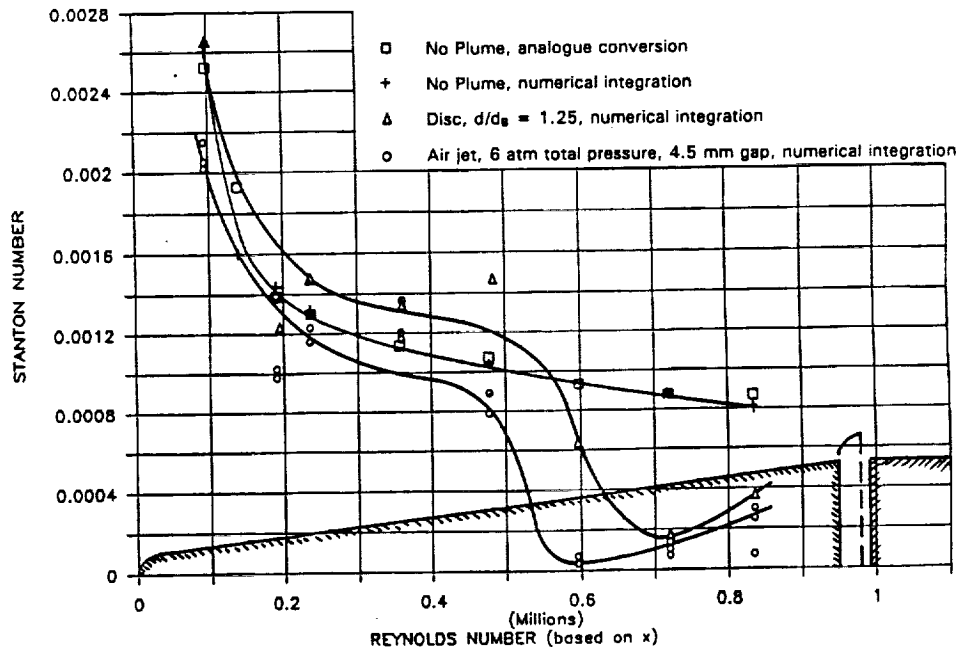
Figure 11. Effect of small-diameter disc and annular air jet on heat transfer to cone surface.
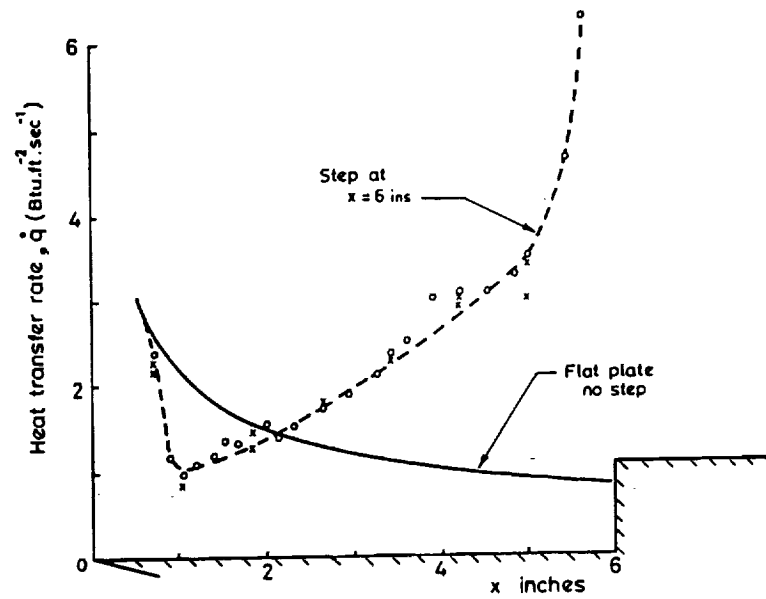
Figure 12. Heat transfer rates in the separated region ahead of a step, $M_\infty = 10$.